American Journal of Civil Engineering
2023; 11(2): 14-25
http://www.sciencepublishinggroup.com/j/ajce
doi: 10.11648/j.ajce.20231102.11
ISSN: 2330-8729 (Print); ISSN: 2330-8737 (Online)

Research on Underground Pipeline Detection Method Based on Background Matrix Subtraction and Three-Dimensional Velocity Spectrum

Haowei Ji, Jian Peng*, Minglei Ma, Jie Ge

Engineering Research Institute, China Construction Eighth Engineering Division Corp., Ltd., Shanghai, China

Email address:

pengjiantj@hotmail.com (Jian Peng)

*Corresponding author

To cite this article:

Haowei Ji, Jian Peng, Minglei Ma, Jie Ge. Research on Underground Pipeline Detection Method Based on Background Matrix Subtraction and Three-Dimensional Velocity Spectrum. *American Journal of Civil Engineering*. Vol. 11, No. 2, 2023, pp. 14-25.
doi: 10.11648/j.ajce.20231102.11

Received: March 17, 2023; **Accepted**: April 6, 2023; **Published**: April 14, 2023

Abstract: Ground-penetrating radar (GPR) can detect urban underground pipelines and image their spatial distribution. However, due to the interference of direct wave and ground reflected wave in radar profile, the detection accuracy of underground pipeline depth is low. In order to improve the reliability and accuracy of the interpretation of ground penetrating radar data, it is necessary to suppress the noise, and then to detect underground pipelines. Firstly, on the basis of data collection, a background matrix subtraction (BMS) method is proposed to suppress noise signals, and the Noise reduction effect is compared and analyzed by two groups of simulation data and two groups of measured data examples with the method of reducing average channel and singular decomposition. Then, a three-dimensional velocity spectrum (3DVS) method is proposed to estimate the buried depth of underground pipeline in radar profile, and the propagation velocity of electromagnetic wave in underground media is calculated by automatically scanning the hyperbolic reflection signal. The estimated velocity is used to carry out back-propagation migration (BPM) processing on the ground penetrating radar profile, and the underground pipeline is accurately detected. Finally, the underground pipeline detection method based on BMS and 3DVS is applied to a residential area in Nanjing, Jiangsu, China. The detection results show that the effect of BMS is obviously better than that of mean-reducing method and singular decomposition method, which can suppress the noise well on the basis of ensuring that the effective signal is not lost. It is helpful to identify the characteristics of target signal in ground penetrating radar profile, and improve the accuracy and reliability of data interpretation. The error between the velocity value estimated by the 3DVS method and the real value is less than 3.8%, and the buried depth error of pipeline target in the obtained data is 1.4%, which indicates that the algorithm has practical application value and can realize the accurate positioning of underground pipelines.

Keywords: GPR, Noise Reduction, BMS, 3DVS, Pipeline Detection

1. Introduction

With the rapid development of cities, the distribution of urban underground pipelines is becoming more and more complicated [1]. At present, due to the age of many old pipelines, lack of management and maintenance and other reasons, detailed information such as pipeline location and burial depth has been missing, which brings hidden dangers to urban construction and construction [2]. Therefore, it is very important for urban construction and development to accurately determine the location and depth of underground pipelines [3]. Ground-penetrating radar (GPR) is widely used in urban underground pipelines due to its high resolution, high efficiency and non-destructive penetrating [4]. GPR is based on high frequency broadband electromagnetic wave to probe underground targets or objects [5, 6]. Compared with other geophysical exploration methods, ground penetrating radar has the advantages of simple operation, high resolution, real-time imaging and strong adaptability [7, 8].

Before detecting underground pipelines, non-target components in radar data need to be removed by suppressing noise signals, so as to enhance target signals and provide basis

for subsequent pipeline detection [9, 10]. At present, radar data Noise reduction methods can be divided into two categories: noise model based and signal statistics based [11-13]. Among them, the method of reducing the average channel based on noise model is more commonly used, but because of the simple calculation method, the Noise reduction effect is not ideal [14-16]. The maximum likelihood estimation method [17-19], Kalman filter method [20, 21], statistical polarization method [22], independent feature analysis [23] and other algorithms based on signal statistics [24] only have a good effect on suppressing the noise generated when the surface is not smooth, and these algorithms are not stable and sensitive to the parameters used.

Then the pipeline detection is carried out on the radar image after denoising, Scholars at home and abroad have carried out a lot of relevant research [25]. Wang et al. proposed the hyperbolic time-history equation and calculated the wave velocity, cylinder radius and burial depth by using the least square method [26]. Cui et al. reconstructed the drainage pipe target in the GPR image through migration reconstruction and sparse reconstruction methods [27]. Yan et al. locate the reflector hyperbola by determining the vertices [28]. Although there have been studies that can use the results of ground penetrating radar to detect underground pipelines, these methods have problems such as high calculation cost, insufficient calculation accuracy and insufficient robustness, and have not been popularized in practical engineering applications [29-31].

In this study, background matrix subtraction (BMS) is proposed to suppress noise signals and accurately detect underground pipelines by three-dimensional velocity spectrum (3DVS) method. is chosen as the study area in Nanjing, Jiangsu, China. This helps to enhance the accuracy and efficiency of pipeline detection. Later, the BMS is compared with the reduction of the average channel method and the singular decomposition method. At the same time, the above three methods are used respectively to detect the reinforced concrete structure and underground pipeline detection of two cases of simulation data and a group of measured data Noise reduction processing, and the results are compared and analyzed.

2. Methodology and Materials

2.1. Noise Reduction Based on BMS

BMS processes radar data as a matrix, and the number of rows and columns of the matrix correspond to the number of sampling points and tracks of radar data respectively. By calculating the background matrix composed only of noise, which is the same size as the radar data matrix, and then subtracting it from the original radar signal matrix, the noise signal is suppressed. The implementation process of BMS includes the following steps:

Arrange Horizontal Windows at each sampling point of the GPR profile data matrix;

Calculate the average value of radar data in the window;

$$A_\alpha = \frac{1}{N-2L}\sum_{i=L+1}^{N-L} a_i \tag{1}$$

$$L = N \times \alpha \tag{2}$$

Where, N is the width of the one-dimensional horizontal window, α is the clipping coefficient, L is the number of data points to be excluded, and a_i is the value of the radar signal corresponding to the data point i.

Keep the radar signal value $\bar{a}_i$ with the same polarity of A_α in the window;

$$\bar{a}_i = \begin{cases} a_i \ \text{sign}(\alpha_i) = \text{sign}(A_\alpha) \\ \text{Null Other circumstances} \end{cases} \tag{3}$$

Where, sign is signal processing.

Weight proximity data W_i;

$$W_i = \frac{1}{(x_i)^s} \tag{4}$$

$$x_i = \sqrt{(\bar{a}_i - A_\alpha)^2} \tag{5}$$

Where, s is weight coefficient, x_i is the degree of data proximity.

Normalize the sample weights $\bar{W}_i$;

$$\bar{W}_i = \frac{W_i}{\sum_{j=1}^{M} W_j} \tag{6}$$

Calculate the background noise A of one-dimensional window data points;

$$A = \sum_{i=1}^{M} \bar{a}_i \times \bar{W}_i \tag{7}$$

Slide the window along the horizontal and vertical directions and assign the element values to the corresponding positions to create a background matrix with the same dimension as the radar data matrix.

2.2. Underground Pipeline Detection Based on Three Dimensional Velocity Spectrum Method

The principle of velocity spectrum analysis method is to assume a series of possible test velocities, calculate the coherence of signals at different offsets or different channels by the hyperbola determined by these test velocities, and then plot the superimposed coherence in the velocity and vertical travel time graph, namely, get the velocity spectrum. When the test velocity is close to the true velocity, the superposition energy peaks in the velocity spectrum, from which the velocity of hyperbolic reflection and the bidirectional vertical

propagation time can be extracted.

Signal coherence is calculated by stacking amplitude;

$$S_{i,j,k} = \sum_{j=1}^{N_i} f\left(t_{i,j,k}, x_j\right) \tag{8}$$

$$i = 1,\cdots,nt; \quad j = 1,\cdots,nx; \quad k = 1,\cdots,nv \tag{9}$$

Where, f is the common offset data in the t-x domain, Ni is the size of the horizontal calculation area selected for the i time, nt, nx and nv are respectively the number of sampling points and tracks of each recording track and the speed number used in the iterative calculation, x_j is the horizontal distance between the point j and the extreme point of the hyperbola, and $t_{i,j,k}$ is the bidirectional time of the point j of the hyperbola.

$t_{i,j,k}$ can be obtained by the following formula;

$$t_{i,j,k} = \left(t_i^2 + \frac{4x_j^2}{v_k^2}\right)^{\frac{1}{2}} \tag{10}$$

Where, ti is the double travel time of the hyperbola vertex, and vk is the speed used in calculation.

In order to solve the problem of incomplete shape of target hyperbola, the superposition amplitude is normalized $C_{i,j,k}$;

$$C_{i,j,k} = \frac{1}{N_i L} \sum_{j=1}^{L+i-1} \frac{S_{i,j,k}^2}{\sum_{j=1}^{N} f^2\left(t_{i,j,k}, x_j\right)} \tag{11}$$

Where, L is the width of the reflection hyperbola in the direction of time, and Ni is different Windows in the longitudinal direction.

In order to suppress interference, soft threshold function $C'_{i,j,k}$ is introduced;

$$C'_{i,j,k} = \begin{cases} C_{i,j,k} - a, & C_{i,j,k} > a \\ 0, & C_{i,j,k} \leqslant a \end{cases} \tag{12}$$

Find the position of the hyperbola vertex along the maximum value of the distance axis, and extract the velocity slice of this position from the 3DVS. The velocity coordinate of the most energetic point in the velocity slice is the propagation velocity of electromagnetic wave in the underground medium.

2.3. Back-Propagation Migration (BPM) Algorithm

In order to locate the subsurface reflection in radar profile to its real position, the BPM algorithm is introduced. The principle of this algorithm is to classify the reflected wave and diffraction wave according to the superposition of the in-phase amplitudes of each recording channel. Figure 1(a) is a schematic diagram of data collected by GPR along the direction of the survey line. Due to the different propagation time of electromagnetic wave scattered by underground targets at different locations, the electromagnetic wave signal received by the receiving antenna is shown as a hyperbola in the radar profile, as shown in Figure 1 (b).

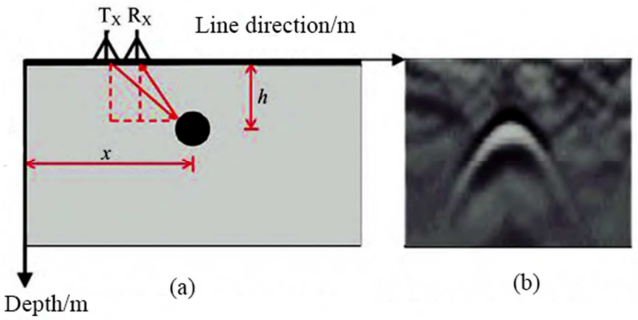

Figure 1. *(a) Ground penetrating radar underground detection principle, (b) Hyperbolic morphology of scattered targets in radar profile data.*

When backpropagation migration is performed on GPR data, the range of the imaging region and the number of pixels are first determined. For each pixel in the imaging space, it is regarded as a scatterer target, and the scattering field corresponding to the pixel is calculated. The calculation steps of the BPM algorithm are as follows:

In uniform underground media, electromagnetic waves transmitted by the transmitting antenna will be reflected when they meet the scatterer target, and will eventually be received by the receiving antenna. The propagation distance R of the whole process is

$$R = \sqrt{\left(T_x - x\right)^2 + h^2} + \sqrt{\left(R_x - x\right)^2 + h^2} \tag{13}$$

Where, Tx and Rx are the positions of transmitting antenna and receiving antenna respectively, h is the underground depth of the target, and x is the distance of the scanning direction of the antenna.

Calculate the propagation time t of electromagnetic wave;

$$t = \frac{\sqrt{\left(T_x - x\right)^2 + h^2} + \sqrt{\left(R_x - x\right)^2 + h^2}}{v} \tag{14}$$

Where v is the propagation speed of electromagnetic wave in the medium.

The receiving amplitudes at each recording time are superposition to obtain the back propagation deviation $s(x,h)$.

$$s(x,h) = \sum_{i=1}^{n} f\left(i,t\right) \tag{15}$$

Where f is the receiving amplitude.

2.4. Numerical Simulation Test

Noise Reduction Simulation

Firstly, the numerical simulation test of reinforcement detection in concrete and underground pipeline detection is carried out, and the simulation data is processed. The simulation model (Figure 2a) is established for the detection of reinforcement in reinforced concrete structures by ground penetrating radar. The model size is 3m× 0.5m, the relative dielectric constant of concrete is 6, and the buried depth of reinforcement is 5cm. The number of discrete grids is 1500×250, and the mesh size is 0.002m. The excitation source uses Riker wavelet with center frequency of 2GHz and sampling time window of 8ns. The finite-difference time-domain method was used for simulation, and 575 signals were obtained with the antenna sending and receiving spacing of 0.05m and the channel spacing of 0.005m. The simulated profile of ground penetrating radar is shown in Figure 2b, from which strong direct wave signal, surface reflection and hyperbolic reflection generated by reinforcement can be seen.

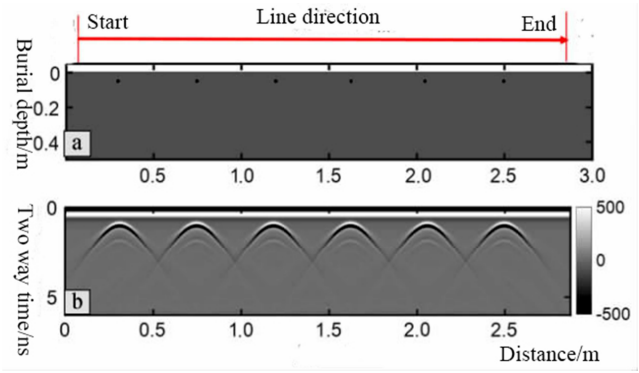

Figure 2. *(a) Reinforced concrete simulation model, (b) reinforced reflection radar profile.*

In order to analyze the Noise reduction effect of BMS, the reduced mean channel method and singular decomposition method are introduced for comparative analysis. The data processing results are shown in Figure 3.

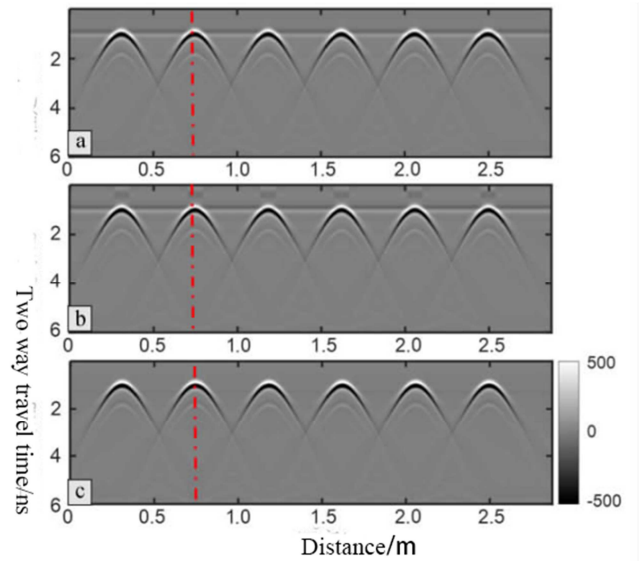

Figure 3. *(a-c) Rebar reflection radar profiles after Noise reduction of three methods.*

BMS is the best method to remove direct wave, and almost no false reflection is generated in the processed image. For the method of reducing the average channel (RAC) and singular decomposition method (SDM), due to the defects of the algorithm, there is a deviation in the calculation of noise signal, which leads to the false signal at the position of the steel bar. Select the position of red dotted line in Figure 3 to draw single-channel signal, as shown in Figure 4.

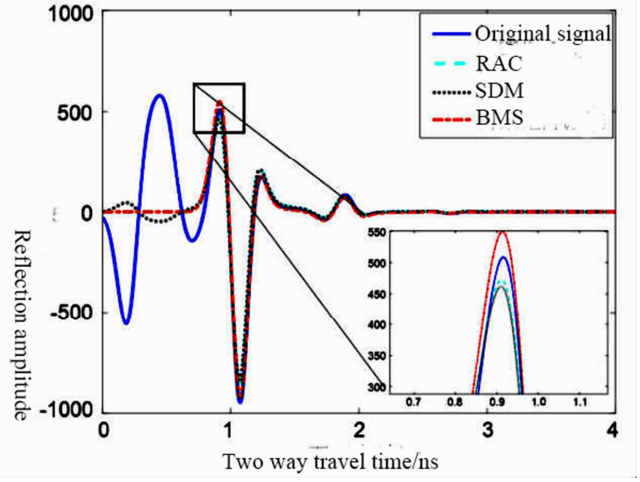

Figure 4. *Single channel reflection signal of reinforcement after Noise reduction.*

After reading the amplitude of the target, the difference between the amplitude calculated by the reduced mean channel method, singular decomposition method and BMS and the original data is -7.2%, -9.2% and 8.2%, respectively. It can be seen that among the three methods, the target signal fidelity after BMS is better, while the other two algorithms will cause attenuation to the target signal.

Figure 5a shows the numerical model of hollow plastic pipeline with layered structure. The GPR profile obtained by simulation is shown in Figure 5b, from which strong direct wave signals, ground reflection, hyperbolic reflection of pipeline and reflection at the layered layer of underground media can be seen. Due to the strong direct wave signal, the reflected signal of the underground pipeline in the radar profile is weak, which is not conducive to our analysis of the characteristics of the underground target, so the data need to be de-noiseed signal processing. In order to compare the Noise reduction effect, the data in Figure 5b are processed by three algorithms, namely, mean-reducing method, singular value decomposition method and BMS, and the results after processing are shown in Figure 6.

Figure 6 shows that different methods can remove direct waves well, but the singular decomposition method and the average channel reduction method have deviation in the calculation of the noise value at the maximum amplitude, and excessive signal removal during Noise reduction results in false signals in the radar profile. However, BMS has the best effect, showing that its suppression results are cleaner and the energy of false signals is lower, especially for false signals around 6ns. In order to further compare the Noise reduction

effect of different methods, the target reflection amplitude is extracted from Figure 5, and the pros and cons of different algorithms are evaluated by calculating the percentage of amplitude change before and after processing. Select the single channel signal reflected by the target at the position of the red dotted line in Figure 5 to draw the comparison diagram of the reflected signal, as shown in Figure 7.

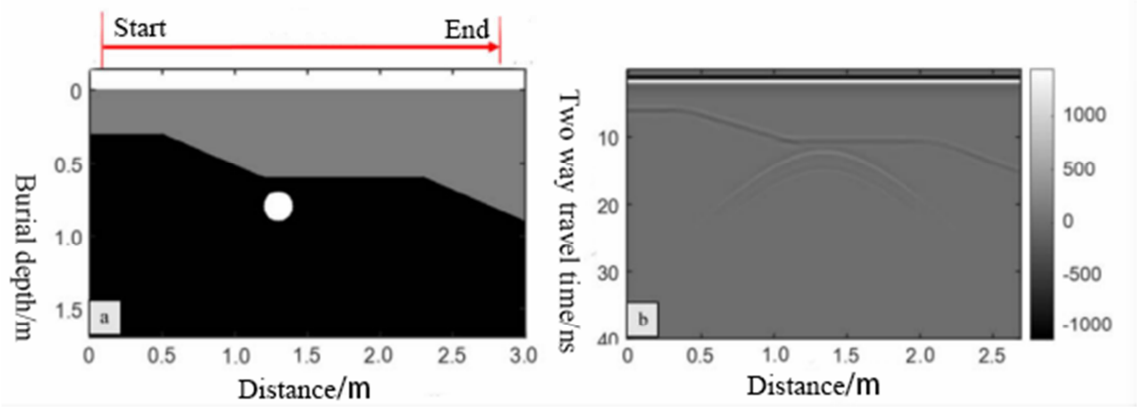

Figure 5. *(a) Pipeline simulation model, (b) reflection Radar Profile.*

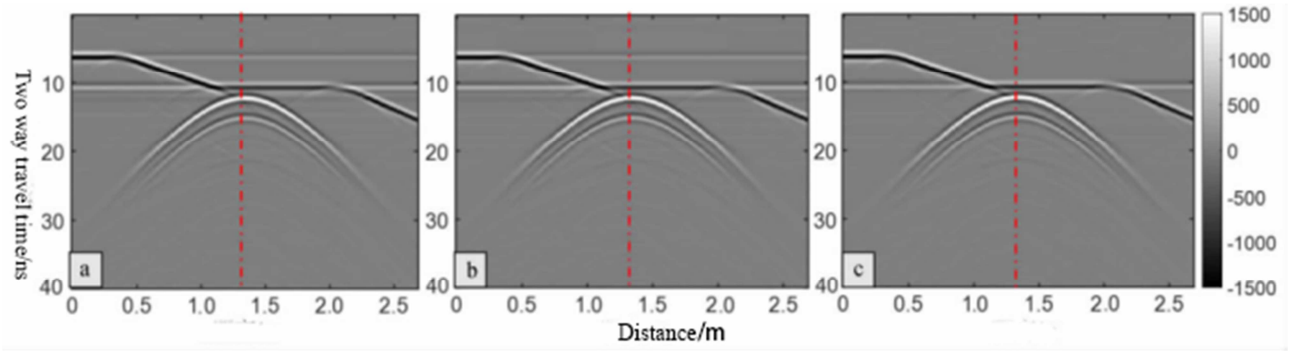

Figure 6. *Radar profile of pipeline reflection after Noise reduction.*

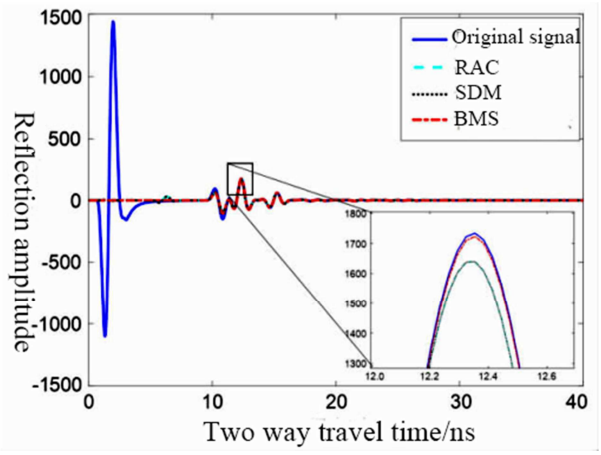

Figure 7. *Single channel reflection signal after Noise reduction.*

After reading the target reflection amplitude from Figure 7, it is found that the target signal is disturbed after processing by the three algorithms. However, the attenuation rate of the target signal amplitude after BMS is 0.5%, which is much lower than that of the other two algorithms, which is 5.4%.

2.5. Underground Pipeline Detection Simulation

In this paper, finite difference time domain method is used for numerical simulation of underground pipeline model. Figure 8 shows the adopted simulation models, all of which are 2 m×1 m in size. The upper layer of Model 1, Model 2, Model 3 and model 4 is homogeneous air layer, and the lower layer is 0.9m thick dry sand, sandy soil, concrete and wet sand respectively. The relative dielectric constants of dry sand, sandy soil, concrete and wet sand are 3.0, 4.5, 6.0 and 8.0, respectively.

A 0.15m diameter metal tube was placed in the center of each model. The grid size of FDTD is set to $\Delta x = \Delta y =$ 0.0025m, and Perfectly Matched Layer (PML) is used for model boundaries. The excitation source uses Ricker wavelet with a center frequency of 400 MHz, and the time window is set to 20ns. The transmitter-receiving antenna spacing is 0.05m, and the antenna step length is 0.02m. The ground penetrating radar profile obtained by simulation contains 90 channels of data.

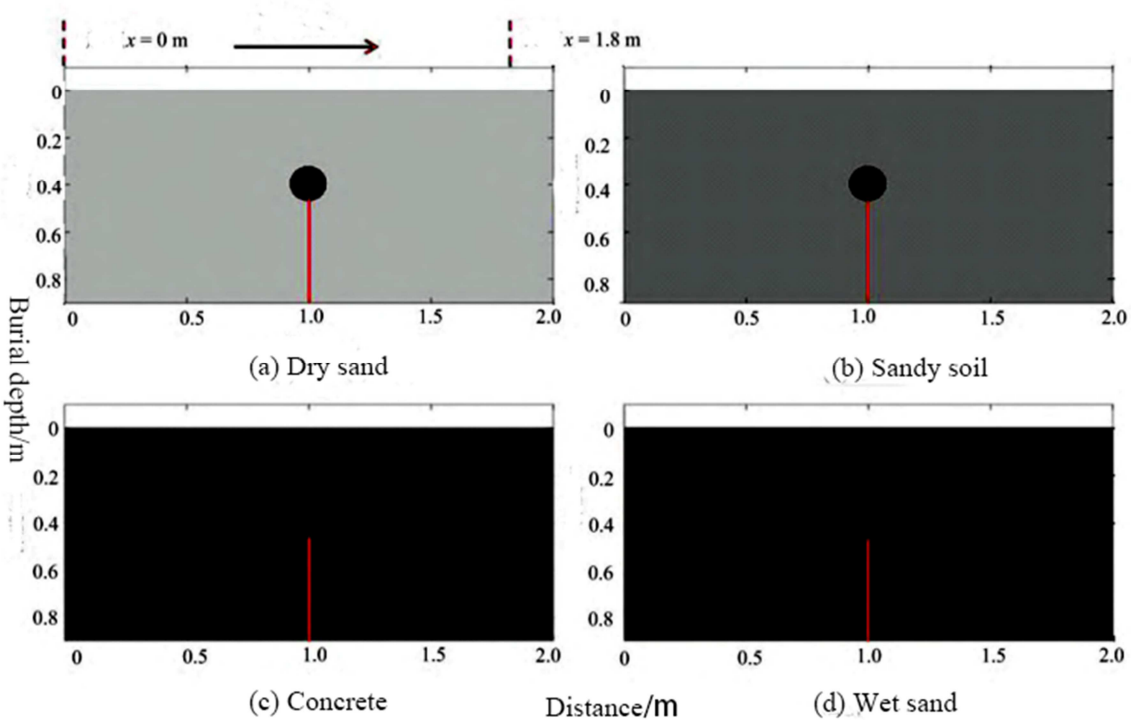

Figure 8. *Simulation model.*

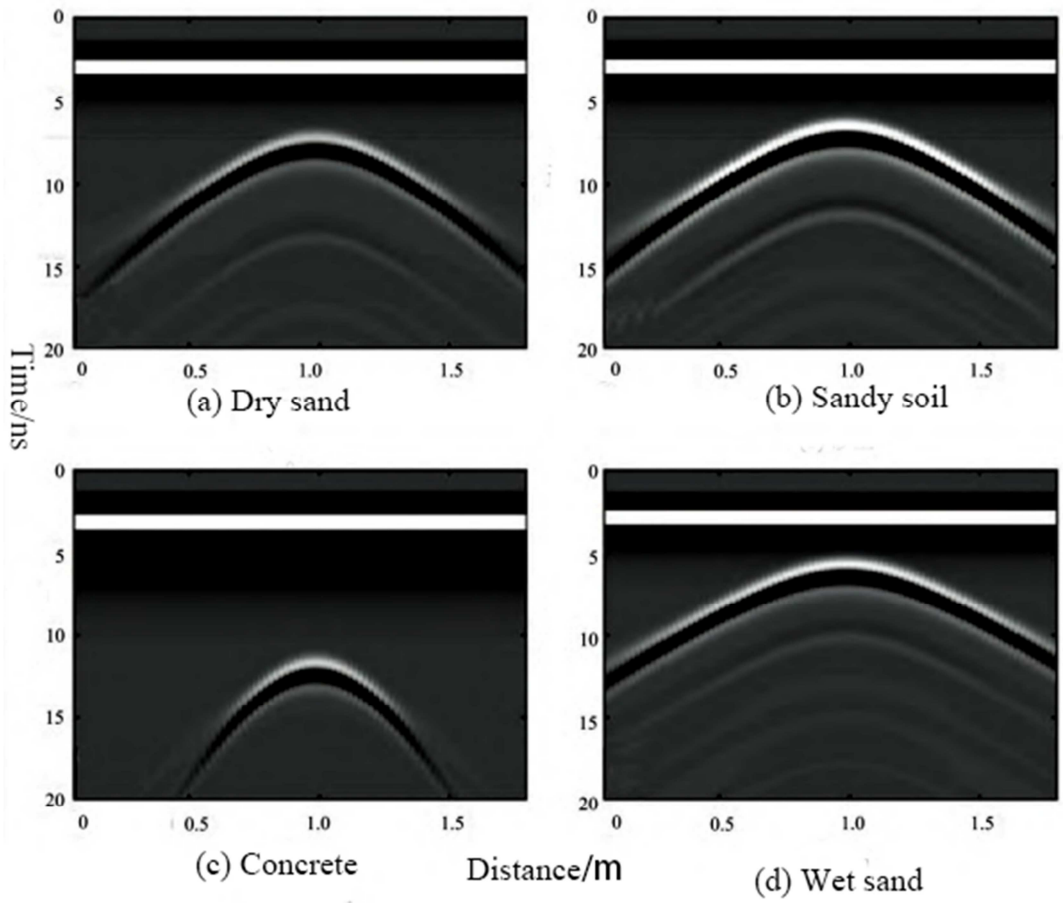

Figure 9. *Simulated radar profile.*

Figure 9 shows the simulated profile of ground penetrating radar, from which the hyperbolic scattering formed by underground targets can be clearly seen. Firstly, the 3D velocity spectrum algorithm is applied to process the ground

penetrating radar data, and the 3D velocity spectrum as shown in Figure 10 is obtained.

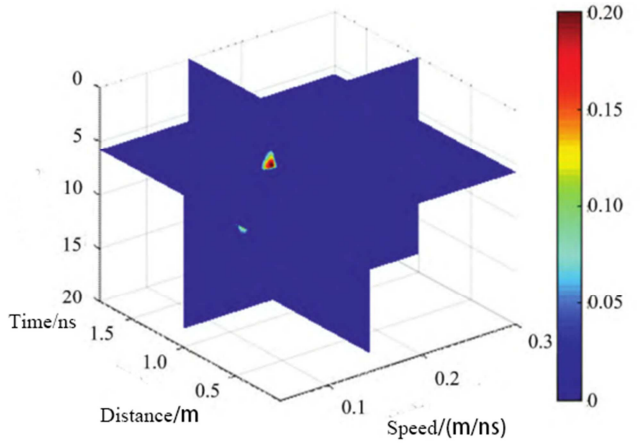

Figure 10. *3DVS results corresponding to the sand model (Figure 3(b)).*

By finding the position of the hyperbola along the maximum value of the distance axis, the velocity slice of this position is extracted from the 3DVS, as shown in Figure 11.

Figure 11 includes the energy block superimposed by hyperbola of underground target scattering. Note that the energy block at 11 ns is formed by hyperbola superimposed by multiple reflected waves. A black "cross" marks the propagation speed of the electromagnetic wave in the medium. Table 1 shows the comparison between the velocities calculated by using the 3DVS method and the real values. It can be seen that the estimated electromagnetic wave velocities have high accuracy, and the errors compared with the real velocities are all less than 3.8%. The calculated propagation velocities were respectively applied to the backward propagation migration algorithm, and the radar profile as shown in Figure 12 was obtained.

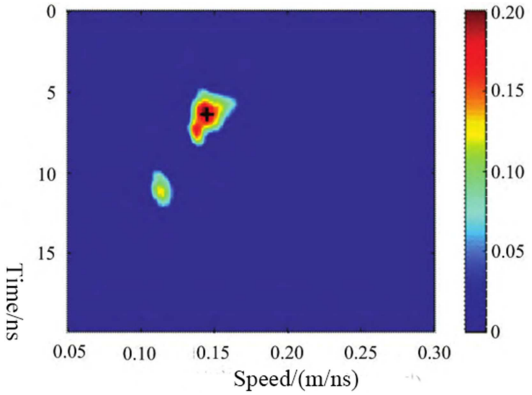

Figure 11. *3DVS slices of sand model.*

Table 1. *The comparison between the velocities calculated by using the 3DVS method and the real values.*

Velocity calculated by 3DVS method/(m/ns)	Real velocity/(m/ns)	Difference value/(m/ns)	Relative error/%
0.1357	0.1401	0.0044	3.140613847
0.1612	0.1586	-0.0026	1.639344262
0.1563	0.1521	-0.0042	2.761341223
0.1257	0.1301	0.0044	3.382013836
0.1423	0.1378	-0.0045	3.265602322
0.1663	0.1622	-0.0041	2.527743527

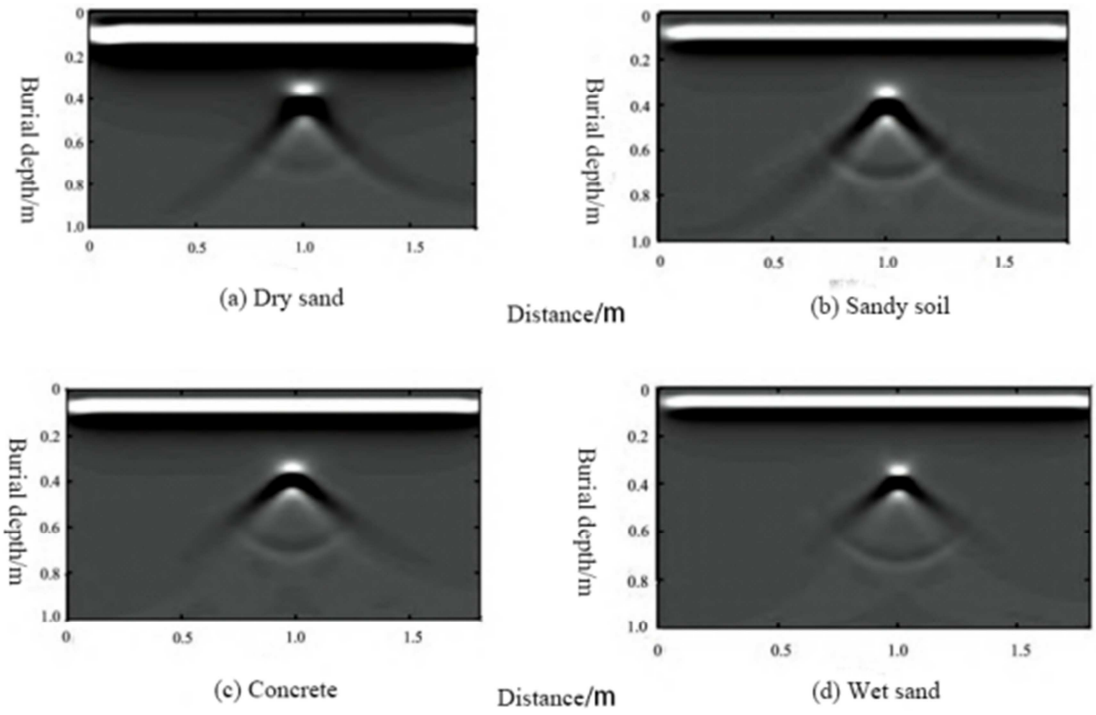

Figure 12. *Simulation data BPM results.*

As can be seen from Figure 12, although the electromagnetic wave propagates at different speeds in each model medium, the diffraction energy generated by the metal tube is well focused. The location of energy focus is the burial depth of the corresponding pipeline. The buried depth of the pipeline obtained from Figure 16 is 0.340, 0.330, 0.330 and 0.335, respectively, with an error of 4.6%, 1.5%, 1.5% and 3.1% from the real buried depth. The simulation results show that the 3DVS algorithm can accurately calculate the wave velocity of electromagnetic wave in underground media and realize the accurate location of underground pipeline.

3. Results and Discussion

3.1. Case Study

The study area takes a residential area in Nanjing, Jiangsu, China as an example. Residential area No. 200, Hankou West Road, Nanjing is an old residential area. Due to the long construction time, there are certain hidden dangers in terms of safety, and public services cannot be effectively guaranteed. The transformation of the old district is to meet the increasing needs of the people, to improve the management of the city, to improve the people's living environment. The transformation of the old residential area not only includes the renovation, reinforcement and beautification of the above-ground part, but also the systematic detection of underground infrastructure such as drainage pipes, underground cables, and water transmission lines, and the corresponding transformation optimization and filing. The test area is located in the residential area, No. 200, Hankou West Road, Gulou District, Nanjing City, Jiangsu Province, as shown in Figure 13.

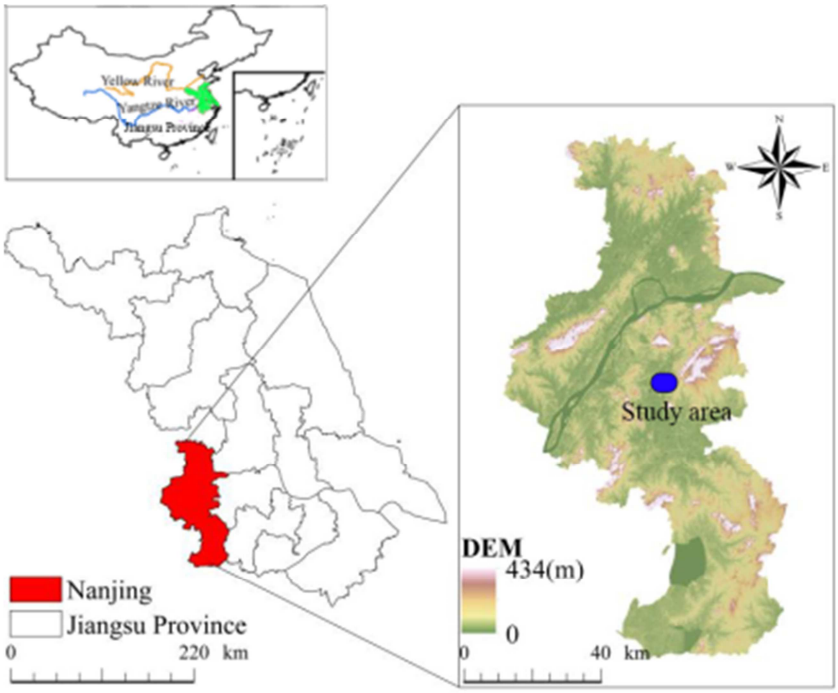

Figure 13. *Geographical location of the test area.*

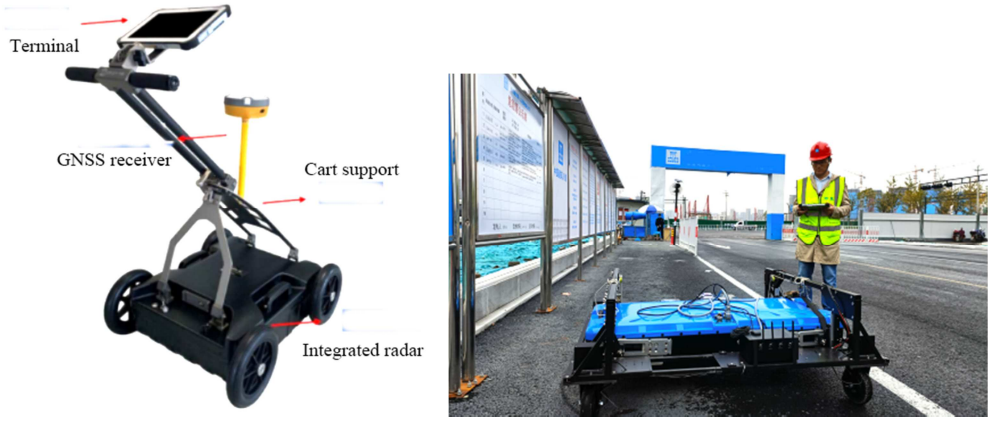

(a) (b)

Figure 14. *(a) High resolution radar 1.0, (b) high resolution radar 2.0.*

The distribution of survey area and survey line in this GPR detection is shown in Figure 15. The main arterial roads in the community are divided into 10 areas (area 8 is located outside the community).

Figure 15. *Ground penetrating radar survey area division and survey line layout.*

Then, high resolution radar is used to collect radar data in the above line area. The collected data contains noise signals. Before detecting underground pipelines, Noise reduction processing is needed.

Noise Reduction

The collected GPR profile of the underground pipeline is shown in Figure 16.

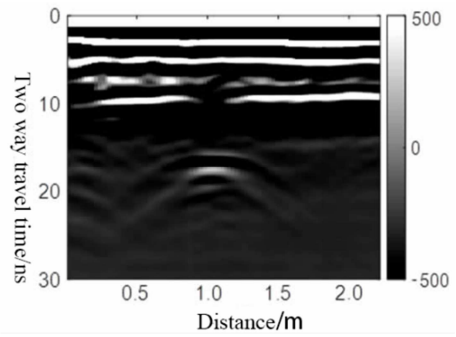

Figure 16. *Pipeline reflection radar profile.*

The hyperbolic reflection signal of underground pipeline cannot be presented clearly because of the strong noise caused by direct wave and uneven background medium. The three Noise reduction algorithms introduced above are used to process the measured data respectively, and the results after processing are shown in Figure 17.

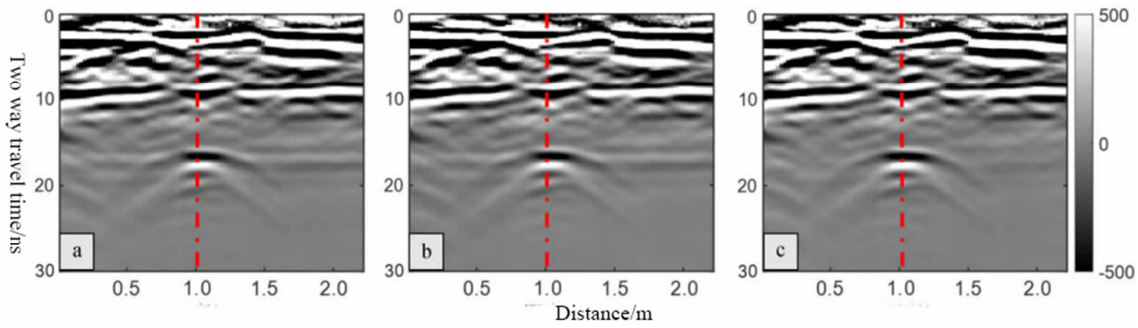

Figure 17. *Radar profile of pipeline reflection after Noise reduction.*

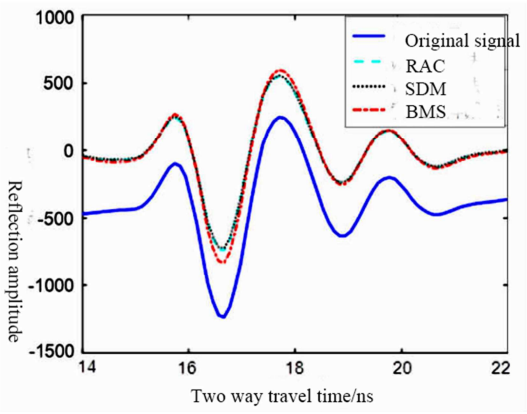

Figure 18. *Single channel reflected signal of pipeline after Noise reduction.*

It can be seen from Figure 17 that the three algorithms have similar effects on noise processing. The direct wave is well removed, which makes the hyperbolic reflection apparent. However, there is false reflection at the vertex position of the target hyperbola in the results processed by the reduced average channel method (Figure 17a) and the singular decomposition method (Figure 17b), which is similar to the results after Noise reduction of the simulation data in the previous paper, while there is no false reflection in the BMS method (Figure 17c). Similarly, the pipeline target single channel signal processed by different algorithms at the position of red dotted line in Figure 17 is drawn, as shown in Figure 18.

After reading the amplitude of the target, it is calculated that the amplitude percentage of the original data processed by the three algorithms, namely, reducing the average channel method, singular decomposition method

and BMS method, is 120%, 123% and 139% respectively. The results show that BMS is superior to the other two methods.

3.2. Underground Pipeline Detection

3DVS algorithm is applied to radar data after noise signal suppression processing to obtain 3DVS, as shown in Figure 19.

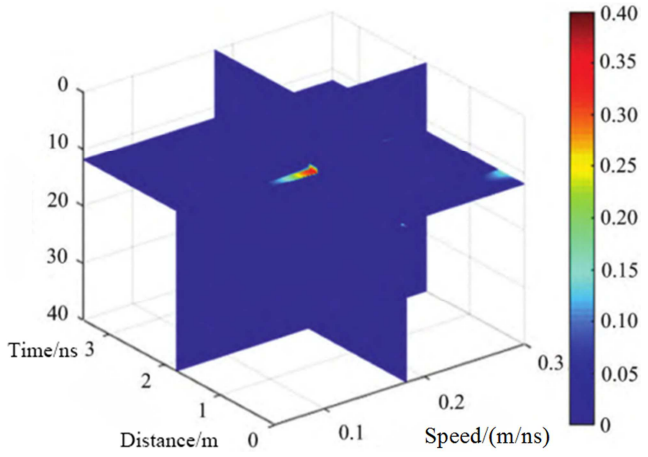

Figure 19. *3DVS of measured data.*

The position of the hyperbola is found through the maximum value along the distance axis, and the velocity slice of the corresponding position is extracted from the 3DVS, as shown in Figure 20.

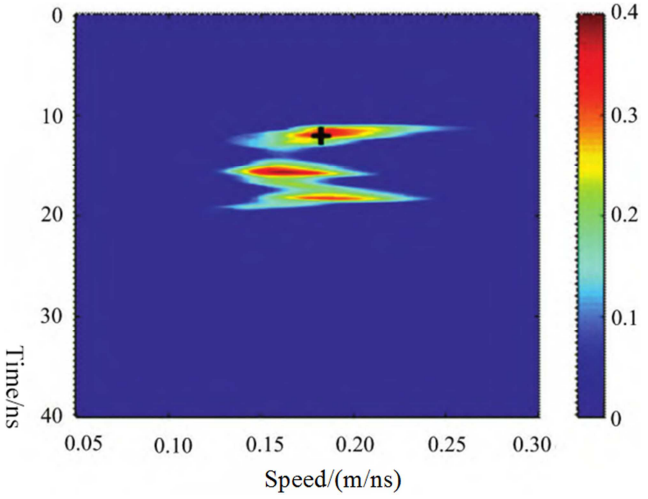

Figure 20. *3DVS velocity slice.*

The black "cross" in Figure 20 is the calculated propagation velocity of electromagnetic wave in the soil medium above the pipe (v= 0.182m /ns). It should be noted that the other two energy blocks are composed of creeping waves and multiple reflected waves. The calculated electromagnetic wave velocity of the soil medium is used for BPM processing of the measured radar data. The results are shown in Figure 21. It can be seen that the scattering formed by the pipeline can be well focused.

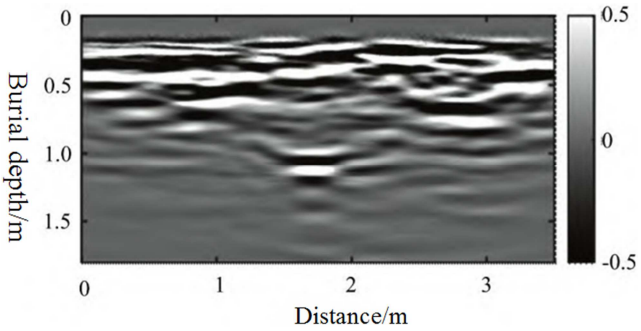

Figure 21. *BPM imaging results of ground penetrating radar data.*

According to Figure 21, it can be clearly positioned that the buried depth of the pipeline is 1.07m. Compared with the actual buried depth of 1.05m, the error is only 1.4%. The actual data results show that the 3D velocity spectrum method also has high accuracy in practical application and can realize the precise location of underground pipeline.

4. Summary and Conclusion

This study aims to use GPR to collect data of underground pipelines in residential areas and to detect them with high accuracy and efficiency. Based on the pipeline data collected, BMS is used to suppress the noise signal, and 3DVS method is used to accurately detect the underground pipeline. By applying the propagation velocity of electromagnetic wave in underground media calculated by 3DVS to the BPM algorithm, the hyperbolic scattering energy of underground pipeline can be focused and the buried depth of underground pipeline can be obtained. In this paper, the method is applied to the detection of underground pipelines in a residential area in Nanjing, Jiangsu, China. Through the research, the main conclusions are as follows:

(1) The effect of BMS is obviously better than that of mean-reducing method and singular decomposition method, which can suppress the noise well on the basis of ensuring that the effective signal is not lost.

(2) It is helpful to identify the characteristics of target signal in ground penetrating radar profile, and improve the accuracy and reliability of data interpretation by using BMS method.

(3) In the numerical simulation model, the error between the electromagnetic wave propagation velocity and the actual velocity calculated by using 3DVS algorithm is less than 3.8%. And in the actual data results, the buried depth error of pipeline target is 1.4%.

(4) The 3DVS algorithm has practical application value and can realize the accurate positioning of underground pipelines.

Data Availability Statement

Some or all data, models, or code that support the findings of this study are available from the corresponding author upon reasonable request.

Funding

Sponsored by Shanghai Pujiang Program.

Acknowledgements

This work was supported in part by the Research on equipment group and technical system of "Four Measurement" in civil engineering (Grant No. 2022-3-15). The authors would like to thank the anonymous reviewers for their constructive comments.

References

[1] Sultanov K S. Parameters of Nonlinear Laws of Longitudinal Interaction of Underground Pipelines with Soil [J]. Soil Mechanics and Foundation Engineering, 2022, 59 (4): 347-353.

[2] Nikolaos A. Behavior of underground energy pipelines under permanent ground displacements [J]. Energy Systems, 2021, 12 (4): 941-954.

[3] Zhou Y, Wang Y, Wu J, et al. Correction to: ErythroidCounter: an automatic pipeline for erythroid cell detection, identification and counting based on deep learning [J]. Multimedia Tools and Applications, 2022.

[4] Li Z, Sun Y, Tian G, et al. Correction to: A compression pipeline for one-stage object detection model [J]. Journal of Real-Time Image Processing, 2021, 18 (6): 1963-1964.

[5] Banerjee A, Banerjee C. A hybrid cellular automata-based model for leakage detection in smart drip irrigation water pipeline structure using IoT sensors [J]. Innovations in Systems and Software Engineering, 2022.

[6] Charvát L, Smrčka A, Vojnar T. Utilizing parametric systems for detection of pipeline hazards [J]. International Journal on Software Tools for Technology Transfer, 2022, 24 (1): 1-28.

[7] Guo C, Shi K, Chu X. Cross-correlation analysis of multiple fibre optic hydrophones for water pipeline leakage detection [J]. International Journal of Environmental Science and Technology, 2022, 19 (1): 197-208.

[8] Zhou Y, Wang Y, Wu J, et al. ErythroidCounter: an automatic pipeline for erythroid cell detection, identification and counting based on deep learning [J]. Multimedia Tools and Applications, 2022, 81 (18): 25541-25556.

[9] Rambika M, Abdalla A T, Maiseli B, et al. Aspect dependent-based ghost suppression for extended targets in through-the-wall radar imaging under compressive sensing framework [J]. EURASIP Journal on Advances in Signal Processing, 2022, 2022 (1): 63.

[10] Xia D, Zhang L, Wu T, et al. A clutter-suppression method for airborne bistatic polarization radar based on polarization-space-time adaptive processing [J]. Multidimensional Systems and Signal Processing, 2022, 33 (3): 899-916.

[11] Zeng L, Zhang Z, Wang Y, et al. Suppression of dense false target jamming for stepped frequency radar in slow time domain [J]. Science China Information Sciences, 2022, 65 (3): 139301.

[12] Galati G, Pavan G, Wasserzier C. Signal design and processing for noise radar [J]. EURASIP Journal on Advances in Signal Processing, 2022, 2022 (1): 52.

[13] Thakur A, Saini D S. Correlation Processor Based Sidelobe Suppression for Polyphase Codes in Radar Systems [J]. Wireless Personal Communications, 2020, 115 (1): 377-389.

[14] Fitasov E S, Kudryashova O E, Legovtsova E V, et al. Coherence of Active Noise Interference in Radar Systems with Antenna Arrays [J]. Radiophysics and Quantum Electronics, 2022, 65 (2): 147-155.

[15] Krysov A V, Raifel D M A. Algorithm for Spatial Filtering of Broadband Signals in a Phased Array Radar Based on Their Decomposition in Interference Space [J]. Optoelectronics, Instrumentation and Data Processing, 2022, 58 (1): 15-23.

[16] Alotaibi M. Low noise moving target detection in high resolution radar using binary codes [J]. EURASIP Journal on Advances in Signal Processing, 2021, 2021 (1): 8.

[17] LeVine M V, Piana-Agostinetti S, Szalay T, et al. TRAMPLE: maximum likelihood estimation of protein unfolding rates from all-atom temperature ramp simulations [J]. Biophysical Journal, 2022, 121 (3S1).

[18] Kong Y S, Abdullah S, Singh S S K. Distribution characterisation of spring durability for road excitations using maximum likelihood estimation [J]. Engineering Failure Analysis, 2022, 134.

[19] Tomio Y, Nagatsuka H. A Conditional Maximum Likelihood Estimation of the COM-Poisson Distribution and its Uniqueness and Existence [J]. Total Quality Science, 2022, 7 (3).

[20] Chengzhong X, Xiaoli L, Kang W, et al. Prediction of outlet pressure for sulfur dioxide blower based on ARX model and adaptive Kalman filter: The 34th China Control and Decision Making Conference [C], Hefei, Anhui, China, 2022.

[21] Lin T, Wenchao X, Long C. Hand Position Tracking based on Optimized Consistent Extended Kalman Filter: The 34th China Control and Decision Making Conference [C], Hefei, Anhui, China, 2022.

[22] Lorena R, Carmen T. Statistical polarization in greenhouse gas emissions: Theory and evidence [J]. Environmental Pollution, 2017, 230.

[23] Fryer D V, Strumke I, Nguyen H. Model independent feature attributions: Shapley values that uncover non-linear dependencies. [J]. PeerJ. Computer science, 2021, 7.

[24] J. C H, G. M, U. R, et al. Using a Regression Ground Clutter Filter to Improve Weather Radar Signal Statistics: Theory and Simulations [J]. Journal of Atmospheric and Oceanic Technology, 2021, 38 (8).

[25] Geng S, Zhu R, Li P, et al. Research on capacitive compensation based on underground pipeline detection system [J]. Journal of Physics: Conference Series, 2022, 2383 (1).

[26] Wang T K, Lin Y H, Shen J Y. Developing and Implementing an AI-Based Leak Detection System in a Long-Distance Gas Pipeline [J]. Advances in Technology Innovation, 2022, 7 (3).

[27] Cui H, Cao J, Hao Q, et al. Omnidirectional ghost imaging system and unwrapping-free panoramic ghost imaging. [J]. Optics letters, 2021, 46 (22).

[28] Wang T, Yan X, Huang Z, et al. Application of pseudo-spectral full waveform inversion in underground pipeline detection [J]. IOP Conference Series: Earth and Environmental Science, 2021, 660 (1).

[29] Xi J, Cui D. Technology of detecting deep underground metal pipeline by magnetic gradient method [J]. IOP Conference Series: Earth and Environmental Science, 2021, 660 (1).

[30] Himri K, Ridao P, Gracias N. Underwater Object Recognition Using Point-Features, Bayesian Estimation and Semantic Information [J]. Sensors, 2021, 21 (5).

[31] Zheng G, Zhao J, Li S, et al. Zero-Shot Pipeline Detection for Sub-Bottom Profiler Data Based on Imaging Principles [J]. Remote Sensing, 2021, 13 (21).